PCCP

COMMUNICATION

The reaction fragility spectrum†

Ludwik Komorowski,*[a] Piotr Ordon[b] and Mateusz Jędrzejewski[a]

We report an original method that provides a new insight into the reaction mechanism by direct observation of bond breaking and formation. Variations of the diagonal elements of the Hessian along the IRC are shown to reflect the anharmonic properties of the system that are induced by electron density modifications upon the reaction. This information is presented in the form of the reaction spectrum, demonstrating how particular atoms engage in the reorganization of bonds. The test reactions are: HCOF synthesis and HONS isomerization.

Introduction

A state-of-the-art review by Klippenstein *et al.*[1] recently summarized the challenges in chemical kinetics and pointed to the role of theory and simulation in this branch of chemistry: computational chemistry often replaces experiment as the primary source of knowledge about the reaction mechanism. Another sensitive point was exposed by Peters[2] who emphasized the useful role of visualization of the atom-by-atom contribution in chemical terms. It may possibly "*foster discovery of new and perhaps simpler ways to understand mechanisms of complex processes*". This communication presents a step along these lines.

An impactful contribution to the computational modelling of the reaction mechanism has been provided by the works of A. Toro-Labbé and P. Politzer *et al.*[3–6] who investigated the energy derivatives over the reaction progress ξ along the IRC: the reaction force ($F_\xi = -\mathrm{d}E/\mathrm{d}\xi$) and the reaction force constant ($k_\xi = \mathrm{d}^2E/\mathrm{d}\xi^2$). These two global quantities have been used to discern tentatively the regions, where the change in geometry or the electron flow is dominating. Results were demonstrated

for a variety of reactions,[7–9] including, sometimes, subtle effects as in the carbocationic rearrangement.[10] The goal of these IRC-based studies was to provide a quantitative description for the qualitative discussions of a reaction mechanism, based on the well-understood properties of the atoms involved. Also, the reaction modelling by the most advanced statistical methods beyond the IRC scheme proved that the atomic-level mechanism may be crucial for the effective reaction course, by allowing for additional energy minima in the reaction channels.[11,12]

The search for the direct role of atoms started with the efforts of Vöhringer-Martinez *et al.*[13] who attributed portions of the activation energy to individual atoms. The sophisticated study of the role of atoms in the reaction run has been presented by Inostroza-Rivera *et al.*[14] The authors chose to decompose the molecular energy into contributions from atomic basins (AIM, Atoms in Molecule proposed by Bader[15]). Simple intramolecular proton transfer reactions (N ↔ H ↔ O) in formamide and in 2-pyridone have been investigated. This complex work led to decomposition of the F_ξ profile into predefined atoms: the moving proton part was dominant, while significant contributions from N and O atoms were mutually compensated. The effect from other atoms could hardly be noticed.

Another approach to unveiling the role of atoms on the reaction path has been proposed in a recent paper from this laboratory.[16] Instead of dividing either the energy, or the density, the atoms have been identified by the actual position of their nuclei ($\mathbf{R}_A$) and the associated Hellmann–Feynman force ($\mathbf{F}_A = -\partial E/\partial \mathbf{R}_A$). This produced straightforward results for the atomic contributions to the reaction force and the reaction force constant [$F_A(\xi)$, $k_A(\xi)$], that are readily computable for each reaction step (ξ):

$$F_A(\xi) = \mathbf{F}_A \cdot \frac{\mathrm{d}\mathbf{R}_A}{\mathrm{d}\xi} \tag{1}$$

$$k_A(\xi) = -\frac{\mathrm{d}F_A(\xi)}{\mathrm{d}\xi} = -\sum_{i \in A}^{x,y,z} \sum_j^{3N} k_{ij} \frac{\mathrm{d}R_i}{\mathrm{d}\xi} \frac{\mathrm{d}R_j}{\mathrm{d}\xi} \tag{2}$$

[a] *Department of Physical and Quantum Chemistry, Wrocław University of Science and Technology, Wyb. Wyspiańskiego 27, 50-370 Wrocław, Poland.*
 E-mail: ludwik.komorowski@pwr.edu.pl
[b] *Department of Physics and Biophysics, Wrocław University of Environmental and Life Sciences, ul. Norwida 25, 50-375 Wrocław, Poland.*
 E-mail: piotr.ordon@up.wroc.pl

32658 | *Phys. Chem. Chem. Phys.*, 2016, **18**, 32658–32663

This journal is © the Owner Societies 2016

Application of the above to a pair of model reactions demonstrated the clear-cut separation of the energy derivatives F_ξ and k_ξ into contributions from atoms. The bond-rupture/formation processes on the reaction steps were reproduced, well in harmony with the variable atomic charges and bond indices (Wiberg[17]). Nonetheless, the numerical results were dominated by the actual change in the position of a nucleus ($d\mathbf{R}_A/d\xi$ factor) as is clear from the definitions (eqn (1) and (2)).

Based on the above results, a novel perspective is opened by this work presenting a method for quantitative monitoring of the variable bonding status of individual atoms as the reaction progresses; the IRC scheme has been explored as the working platform.

Theoretical method

From the chemical point of view, it is more instructive to observe the effects of evolution in the electronic structure of the participating atoms, rather than the collective vibrational modes. The valuable information concerning bonded atoms is buried under the $\mathbf{F}_A$ values, as the Hellmann–Feynman force calculated for atoms for each step of the reaction reflects the structure of the density adjusted to the external potential, according to the Hohenberg–Kohn theorem.[18] The working formula describing the atomic contribution in the reaction force constant (eqn (2)) hints at the elements of the Hessian, from which this information can be extracted:

$$k_{ij} = -\left(\frac{\partial F_j}{\partial R_i}\right)_N = \left(\frac{\partial^2 E}{\partial R_i \partial R_j}\right)_N \quad (3)$$

In a system of N atoms, k_{ij} are elements of the $3N \times 3N$ matrix calculated for each step of the reaction path; R_i and R_j stand for the R_x, R_y, R_z coordinates of each atom.

Let us imagine a molecule with all bonds being harmonic oscillators coupled into the normal modes. Whatever its excitation due to the increasing vibrational energy at moderate atomic amplitudes, the Hessian would not be altered. Hence, its trace (invariant of the matrix) would not change. Should just one mode become dissociative (low dissociation energy in the Morse model), a specific atom involved might be let loose at some excitation energy; its share in the trace would disappear. This would have an effect on other bonds in this hypothetical entity; its electronic structure will change (even if its geometry would not), and the frequencies of its vibrational modes will be altered. The contributions to the trace from atoms remaining in the system will be modified according to their new bonding situation that reflects the reorganized electron density. This example demonstrates that the information regarding the structural evolution of a real system of atoms is hidden in the trace of the Hessian matrix. By applying the model to a simple diatomic molecule we get a hint that reducing the trace corresponds to losing a bond. On the other hand, this also means increasing the anharmonicity as conventionally described by the Morse curve.

The diagram below shows an excerpt of a Hessian, where atoms (A,B) and the coordinates (x,y,z) have been marked:

$$
\begin{bmatrix}
k_{xx}^{AA} & k_{yx}^{AA} & k_{zx}^{AA} & \cdots & & \cdots & & \cdots \\
k_{xy}^{AA} & k_{yy}^{AA} & k_{zy}^{AA} & & & & & \\
k_{xz}^{AA} & k_{yz}^{AA} & k_{zz}^{AA} & & & & & \cdots \\
k_{xx}^{AB} & k_{yx}^{AB} & k_{zx}^{AB} & k_{xx}^{BB} & k_{yx}^{BB} & k_{zx}^{BB} & & \\
k_{xy}^{AB} & k_{yy}^{AB} & k_{zy}^{AB} & k_{xy}^{BB} & k_{yy}^{BB} & k_{zy}^{BB} & & \\
k_{xz}^{AB} & k_{yz}^{AB} & k_{zz}^{AB} & k_{xz}^{BB} & k_{yz}^{BB} & k_{zz}^{BB} & \cdots & \cdots \\
\cdots & & & & & \cdots & \cdots & \cdots \\
\cdots & & & & & \cdots & \cdots & k_{zz}^{NN}
\end{bmatrix}
= \mathbf{K}
$$

The square matrix blocks along the $\mathbf{K}$ matrix′ diagonal describe each individual atom only. Their traces are also invariant upon the rotation or shift of the coordinate system. Hence, the invariant trace of the $\mathbf{K}$ matrix is additively composed by contributions from invariant traces of block atomic matrices $\mathbf{k}^A$:

$$\mathrm{Tr}\,\mathbf{K} = \sum_A^{\text{atoms}} \mathrm{Tr}\,\mathbf{k}^A = \sum_A^{\text{atoms}} \sum_{i \in A}^{x,y,z} k_{ii}^{AA} \quad (4)$$

The evolution of an array of atoms (other than purely harmonic deformation) will mark its effect both on $\mathrm{Tr}\,\mathbf{K}$ and some $\mathrm{Tr}\,\mathbf{k}^A$. This calls for an analytical tool to appreciate the variation in the trace of a Hessian. The most natural candidate is the derivative:

$$a_\xi = \frac{d}{d\xi}(\mathrm{Tr}\,\mathbf{K}) = \sum_A^{\text{atoms}} \frac{d}{d\xi}(\mathrm{Tr}\,\mathbf{k}^A) = \sum_A^{\text{atoms}} a_\xi^A \quad (5)$$

This derivative is well founded: the third energy derivative is related to the anharmonicity of a molecular oscillator.[19–21] Density functional theory analysis of the anharmonicity of molecular oscillators demonstrated its relation to important descriptors of the electronic system, especially the electronic softness that is closely related to the electronic polarizability of the system.[22,23]

The atomic derivative proposed in eqn (5) (a_ξ^A) reports variation in the diagonal elements of the Hessian, with no direct relation to the actual displacement of atoms:

$$a_\xi^A = \frac{d}{d\xi}(\mathrm{Tr}\,\mathbf{k}^A) = \sum_{i \in A}^{x,y,z} \frac{dk_{ii}^{AA}}{d\xi} \quad (6)$$

The changes in the trace elements on the reaction paths result from the evolution of the share of particular atoms in the vibrational energy of a system. This comes as an effect of misplacement of the nuclei on the reaction path, and the electronic reorganization that follows. The bonds are modified accordingly, as reflected by the Wiberg indices.[16] Hence, the density changes are associated with the change in the atomic shares in the trace of the Hessian. a_ξ^A (eqn (6)) is nonzero whenever the vibrational motions of atoms are affected by the electron density redistribution. a_ξ^A would vanish when nothing but harmonic vibrations occur. $a_\xi^A < 0$ reproduces the dissociative effect ($\mathrm{Tr}\,\mathbf{k}^A = 0$ means the atom A forms no bonds at all); the bond formation by an atom is manifested by $a_\xi^A > 0$. Summing the traces over appropriate atoms naturally produces a_ξ indices for chemical groups.

This journal is © the Owner Societies 2016

Phys. Chem. Chem. Phys., 2016, **18**, 32658–32663 | **32659**

Deciphering quantitative information hidden in a_ξ can be achieved using the methods of conceptual density functional theory.[18–20,26] The crucial condition for the analysis is to allow for direct density flow between atoms. This precludes applying the standard regime in the conceptual DFT (constant N) to an atom-in-molecule. The derivatives over $d\xi$ may not be calculated at constant μ either, as the chemical potential varies between the steps on IRC. The simplest solution is to explore the standard DFT procedures applied to an atom-in-molecule, with the variables chosen accordingly: N_A stands formally for the number of electrons associated with an atom and ξ is a unique parameter that replaces the external potential for each configuration along the defined IRC. Thus, by writing the differential dk^A for the trace of an atomic matrix block (in the simplified notation $k^A \equiv \mathrm{Tr}\,\mathbf{k}^A$), the following meaningful result is obtained for the atomic fragility parameter a_ξ^A.

$$a_\xi^A \equiv \frac{dk^A}{d\xi} = \left(\frac{\partial k^A}{\partial \xi}\right)_{N_A} + \left(\frac{\partial k^A}{\partial N_A}\right)_\xi \frac{dN_A}{d\xi} \qquad (7)$$

The first term reflects only the geometry variations of the system (eqn (8)); it is determined by the classical anharmonicity parameters a_{iip} amply discussed in the past,[20] and defined as if there were no exchange of electrons involving atom A in its motions. Hence, it does not contain directly any factors describing the electron flow to or from an atom:

$$\left(\frac{\partial k^A}{\partial \xi}\right)_{N_A} = \sum_p^{3N} \sum_{i\in A}^{x,y,z} a_{iip} \frac{dR_p}{d\xi} \quad \text{where } a_{iip} = \left(\frac{dk_{ii}^A}{dR_p}\right)_{N_A} \qquad (8)$$

The key element within the fragility parameter a_ξ^A is the second term in eqn (7), that contains the joint effect of change in the number of electrons on an atom $dN_A/d\xi$, and the corresponding modification (increase or decrease) of $\mathrm{Tr}\,\mathbf{k}^A = k^A$ that serves as a measure of the connection of that atom with the rest of a system. Eqn (7) and (8) reveal the physical meaning of the atomic fragility parameters.

Results and discussion

The IRC energy profile has been reproduced by the standard procedure at the MP2 level using the 6-311++G(3df,3pd) basis set and the Gaussian 09 code.[24] The number of computational points on the reaction path was 87 for HF/CO and 98 for H/ONS reactions with the standard step of reaction progress $\Delta\xi$ equal to 0.10 and 0.05 respectively.

The evolution of the trace of the Hessian $\mathrm{Tr}\,\mathbf{K}$ for two model reactions is presented in Fig. 1. Eqn (7) is very neatly reflected in the diagrams. The slope of the linear sections at the initial and final periods, where supposedly little electron exchange occurs, determines the constant geometrical parameter, eqn (8). The central, non-linear section of the diagram describes the effects of the electron exchange in the system.

For the H/ONS isomerization far from the transition state (TS, $\xi = 0$), the trace of the Hessian is a linear function decreasing towards the equilibrium structures at both ends. A similar effect is evidenced by the initial part of the curve for HF/CO.
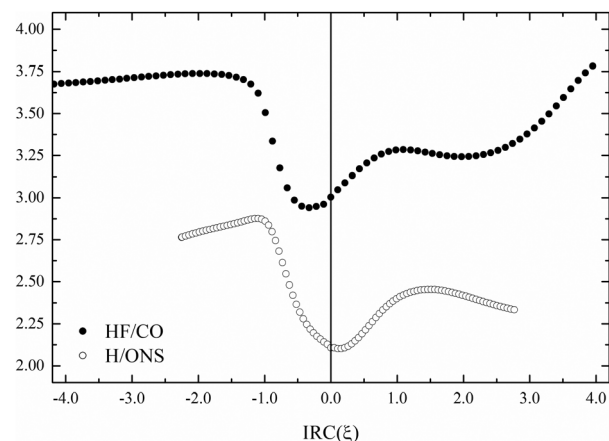

Fig. 1 Variation of the trace of the Hessian matrix $\mathrm{Tr}\,\mathbf{K}$ (eqn (4), atomic units) along the reaction coordinate for the reactions: HF + CO → HCOF and HONS → ONSH.

However, here the meaningful changes in the trace, though concentrated around the TS, extend far beyond the TS region, as marked by the extrema of the reaction force[3,5] (see ref. 25 for the details).

An aftermath of the reaction is evidenced in the region, where significant changes in the geometry have supposedly been completed ($\xi > 3$). The effect is not unexpected: calculated bond lengths, atomic charges and the Wiberg bond indices substantiated a faint suggestion in previous work that the F–C bond formation could be a late second stage of this reaction.[16] The evolution of softness and polarizability for the reacting entity in HF/CO reaction has also been a subject of separate studies,[25–27] and an unexplained plateau on the electronic dipole polarizability dependence on the IRC has been reported in the same region ($\xi > 3$).

Computational results for the derivatives introduced in eqn (5) and (6) have been presented jointly in Fig. 2 and 3. Separate diagrams for atoms and groups with the position of peaks marked have been included in the accompanying ESI.† Inspection of the diagrams in atomic resolution (Fig. 2a and 3a) shows a striking feature: the peaks are grouped in pairs reflecting the bonds – either breaking or those being created. For the HF/CO reaction, the joint destabilizing effect on H and F atoms creates the reaction onset ($\xi = -0.88$, Fig. 2a) and must be interpreted as H–F dissociation, which is confirmed by the Wiberg index decrease.[16] It is preceded with a small strengthening effect on the CO group ($\xi = -1.43$). The second step of this reaction, now fully revealed, is the H–C bond formation ($\xi = 0.0$–0.2). The carbon atom plays the leading role, as a_ξ^{CO} of the CO group also increases ($\xi = 0.21$, Fig. 2b) and despite the slight negative effect introduced by the oxygen in this region (Fig. 2a). The joint adaptation in the HCO moiety ($-0.5 < \xi = 1.0$) may explain the observation from the Wiberg indices:[16] H–C bond is formed first ($-1.0 < \xi = 0$) with the following effect on CO ($\xi > 0$). The tiny oxygen effect must be important for the C–F bond formation in the third step of the reaction, as it does not start until the minimum a_ξ^{CO} is reached at $\xi = 1.53$ (Fig. 2b). The C–F bond is formed at $\xi = 3.40$–3.51, and only
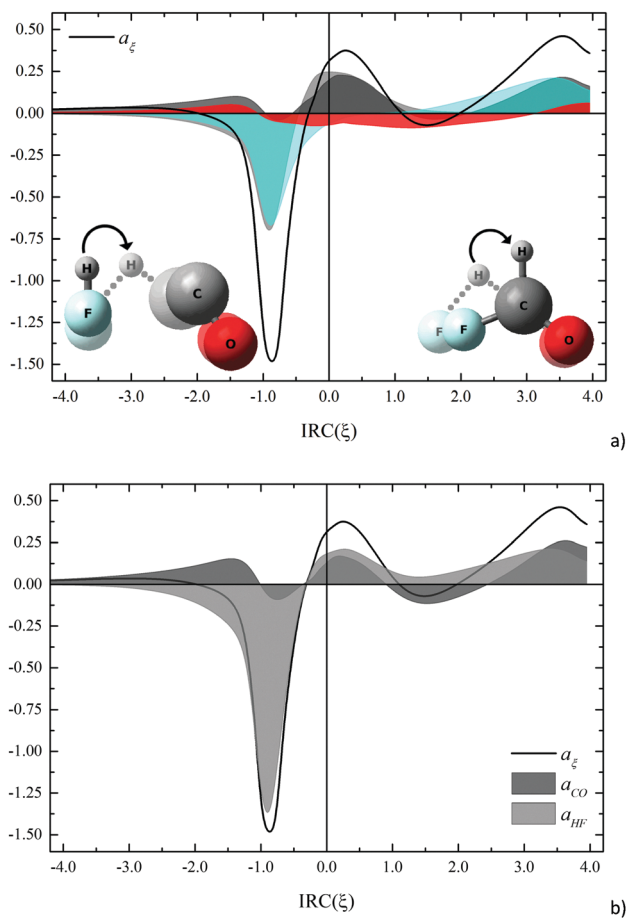
32660 | *Phys. Chem. Chem. Phys.*, 2016, **18**, 32658–32663

This journal is © the Owner Societies 2016

Fig. 2 Decomposition of the derivative a_ξ (eqn (5), solid line, atomic units) for the reacting system HF + CO → HCOF into contributions from atoms (a, colours) and groups (b, shadows), (eqn (6)). Note the effect of transparency in overlapping colours.
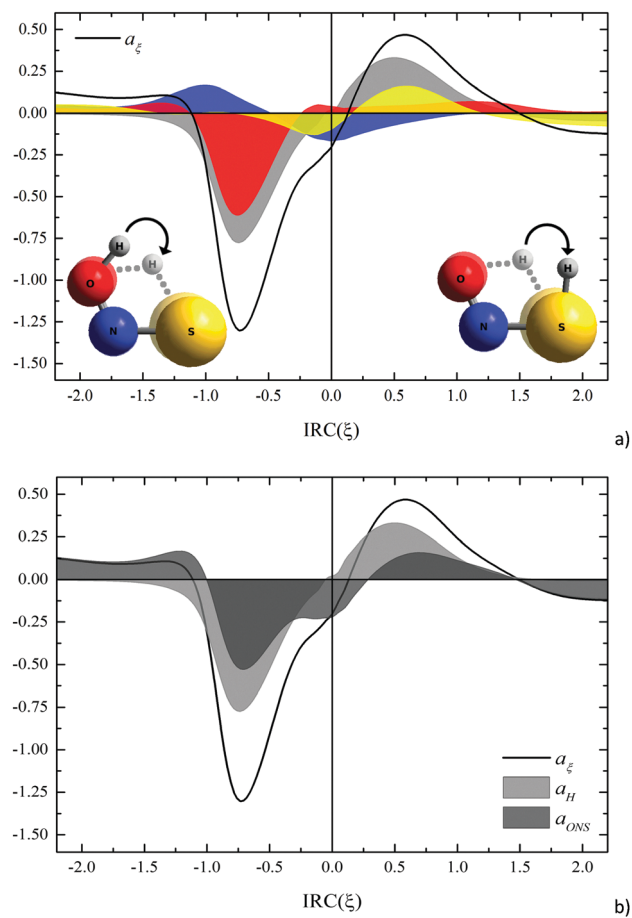

Fig. 3 Decomposition of the derivative a_ξ (eqn (5), solid line, atomic units) for the reacting system HONS → ONSH into contributions from atoms (a, colours) and groups (b, shadows), (eqn (6)). Note the effect of transparency in overlapping colours.

then does the CO bond tend to complete the stabilization of the system. Fig. 2 brings an explanation for the far-from-TS-effects reported in a previous work.[16]

The H/ONS isomerization occurs by proton migration, and no other effects have ever been reported in previous works.[4,13,28,29] Fig. 3 confirms this, but now shows additional reorganization taking place within the ONS moiety. In fact, a slight strengthening of the O–N bond appears to be the initiation of the whole process ($\xi = -1.36$, Fig. 3a). Breaking the H–O bond that occurs at $\xi = -0.73$, well before the TS, is associated with the increasing role of nitrogen (Fig. 3a).

The N–S bond is weakened at the transition state as the 3rd step of this reaction (Fig. 3a). Finally, formation of the H–S bond takes place ($\xi = 0.52$–0.57) and tiny adjustments in O–N–S complete the reaction. The small activity going on at the TS is corroborated by the group diagram in Fig. 3b. The destabilizing effect in the ONS group at TS is clearly demonstrated; it is even noticed on the global curve a_ξ. The detailed picture provided by what we are calling the atomic fragility parameter a_ξ^A does not contradict the coarse information obtained from the Wiberg indices and atomic charges changing along the IRC.[16] They are not quite parallel, covering the range ($-1.0 < \xi < 1.0$), with the

inflection points for the H–O and N–S Wiberg indices preceding TS ($\xi \cong -0.4$), while the central point for the charge on ONS group variation (equal to the negative charge H) was at ($\xi \cong +0.2$).[16]

Looking for some numerical results, the $a_\xi = 0$ points may be considered as reasonable indicators separating the sequences of changes in the bonding status of atoms, with no direct relation to the change in the geometry of the reacting system. The integration of a selected peak in the spectrum produces an atomic fragility index (Δk^A) for a reaction step around the peak maximum. By neglecting the first term in eqn (7) and introducing the average for the derivative $(\partial k^A / \partial N^A) \cong \bar{\lambda}^A$ a crude integration leads to the result:

$$\Delta k^A \equiv k^A(\xi_2) - k^A(\xi_1) = \int_{\xi_1}^{\xi_2} a_\xi^A \, \mathrm{d}\xi$$

$$\cong \int_{\xi_1}^{\xi_2} \left(\frac{\partial k^A}{\partial N_A} \right)_\xi \frac{\mathrm{d}N_A}{\mathrm{d}\xi} \mathrm{d}\xi \cong \bar{\lambda}^A \cdot [N_A(\xi_2) - N_A(\xi_1)] = \bar{\lambda}^A \cdot \Delta N_A$$

$$(9)$$

The average derivative $\bar{\lambda}^A = \Delta k^A / \Delta N^A$ may now be estimated.

For atoms on the reaction path it represents an atomic analogue of the derivative recognized as the mode softening index.[19–21,26] The calculated results are shown in the ESI.†

The essential feature of the proposed reaction spectrum and its theoretical interpretation provide a way to observe how the ongoing reaction affects an individual atom in a reacting system. There is no need to specify the boundaries for the atoms within, since the observation is focused on a quantity (Tr $\mathbf{k}^A = k^A$) not directly dependent on the atomic charge, though sensitive to its variation ΔN_A. Therefore, the reaction spectrum appears to be a suitable tool for the observation of a molecular system's evolution.

In seeking an appropriate name for the third energy derivatives a_ξ, a_ξ^A the terms reaction or atomic fragility seem to represent properly its content: high values hint at atoms whose bonds actually break or form on the collective stretch of a system on a selected step of the reaction path. The further the reacting system is from electronic stability, the larger is the $|a_\xi^A|$ value. The term fragility has been commonly used in chemistry (biochemistry, polymer science) in a similar sense, but has not been defined rigorously.

It may be important to note that calculations of the reaction fragility parameters are not necessarily bound to the IRC formalism. As for the Hessian matrix itself, it can be calculated for any geometrical configuration of the nuclei, thus providing a tool for the observation of the role of atoms on an arbitrarily chosen reaction trajectory.

Conclusions

Bond breaking and formation along the reaction path is clearly reproduced by what we call the "atomic fragility" parameter representing the "reaction fragility" attributed to an atom. The analysis provides an attractively simple, and yet very informative visualization revealing the role of atoms in the density modifications occurring in subsequent reaction steps. The fragility diagrams have the characteristics of spectra, including their facile decomposition into atomic/group components.

Acknowledgements

References

1 S. J. Klippenstein, V. S. Pande and D. G. Truhlar, *J. Am. Chem. Soc.*, 2014, **136**, 528–546.

2 B. Peters, *J. Phys. Chem. B*, 2015, **119**, 6349–6356.

3 J. Martinez and A. Toro-Labbé, *J. Math. Chem.*, 2009, **45**, 911–927.

4 P. Jaque, A. Toro-Labbé, P. Politzer and P. Geerlings, *Chem. Phys. Lett.*, 2008, **456**, 135–140.

5 A. Toro-Labbé, S. Gutiérrez-Oliva, P. Politzer and J. S. Murray, in *Chemical Reactivity Theory. A density functional Viewpoint*, ed. P. K. Chattaraj, CRC Press, Taylor & Francis Group, Boca Raton, U.S.A., 2009.

6 P. Politzer, A. Toro-Labbé, S. Gutiérrez-Oliva and J. S. Murray, in *Advances in Quantum Chemistry*, ed. J. R. Sabin and E. J. Brändas, Elsevier, Amsterdam, N.L., 2012, vol. 64.

7 A. Toro-Labbé, S. Guitiérrez-Oliva, M. C. Concha, J. S. Murray and P. Politzer, *J. Chem. Phys.*, 2004, **121**, 4570–4576.

8 B. Herrera and A. Toro-Labbé, *J. Phys. Chem. A*, 2007, **111**, 5921–5926.

9 V. Labet, C. Morell, A. Toro-Labbé and A. Grand, *Phys. Chem. Chem. Phys.*, 2010, **12**, 4142–4151.

10 D. E. Ortega, S. Guitiérrez-Oliva, D. J. Tantillo and A. Toro-Labbé, *Phys. Chem. Chem. Phys.*, 2015, **17**, 9771–9779.

11 L. Sun, K. Song and W. L. Hase, *Science*, 2002, **296**, 875–878.

12 J. G. Lopez, G. Vayner, U. Lourderaj, S. V. Addepalli, S. Kato, W. A. deJong, T. Windus and W. L. Hase, *J. Am. Chem. Soc.*, 2007, **129**, 9976–9985.

13 E. Vöhringer-Martinez and A. Toro-Labbé, *J. Phys. Chem. A*, 2012, **116**, 7419–7423.

14 R. Inostroza-Rivera, M. Yahia-Ouhmed, V. Tognetti, L. Joubert, B. Herrera and A. Toro-Labbé, *Phys. Chem. Chem. Phys.*, 2015, **17**, 17797–17807.

15 R. F. W. Bader, *Atoms in Molecules. A Quantum Theory*, Clarendon Press, Oxford, U.K., 1990.

16 M. Jędrzejewski, P. Ordon and L. Komorowski, *J. Phys. Chem. A*, 2016, **120**, 3780–3787.

17 I. Mayer, *J. Comput. Chem.*, 2007, **28**, 204–221.

18 R. G. Parr and W. Yang, *Density-Functional Theory of Atoms and Molecules*, Oxford University Press, Oxford, U.K., 1989.

19 P. Ordon, *Effect of Molecular Deformation on the Chemical DFT indices*, PhD thesis, Wrocław University of Technology, 2003.

20 P. Ordon and L. Komorowski, *Int. J. Quantum Chem.*, 2005, **101**, 703–713.

21 L. Komorowski and P. Ordon, *Int. J. Quantum Chem.*, 2004, **99**, 153–160.

22 A. Vela and J. L. Gazquez, *J. Am. Chem. Soc.*, 1990, **112**, 1490–1492.

23 L. Komorowski, J. Lipiński and P. Szarek, *J. Chem. Phys.*, 2009, **131**, 124120.

24 M. J. Frisch, G. W. Trucks, H. B. Schlegel, G. E. Scuseria, M. A. Robb, J. R. Cheeseman, J. A. Montgomery Jr., T. Vreven, K. N. Kudin, J. C. Burant, J. M. Millam, S. S. Iyengar, J. Tomasi, V. Barone, B. Mennucci, M. Cossi, G. Scalmani, N. Rega, G. A. Petersson, H. Nakatsuji, M. Hada, M. Ehara, K. Toyota, R. Fukuda, J. Hasegawa, M. Ishida, T. Nakajima, Y. Honda, O. Kitao, H. Nakai, M. Klene, X. Li, J. E. Knox, H. P. Hratchian, J. B. Cross, C. Adamo, J. Jaramillo, R. Gomperts, R. E. Stratmann, O. Yazyev, A. J. Austin, R. Cammi, C. Pomelli, J. W. Ochterski, P. Y. Ayala, K. Morokuma, G. A. Voth, P. Salvador, J. J. Dannenberg,

V. G. Zakrzewski, S. Dapprich, A. D. Daniels, M. C. Strain, O. Farkas, D. K. Malick, A. D. Rabuck, K. Raghavachari, J. B. Foresman, J. V. Ortiz, Q. Cui, A. G. Baboul, S. Clifford, J. Cioslowski, B. B. Stefanov, G. Liu, A. Liashenko, P. Piskorz, I. Komaromi, R. L. Martin, D. J. Fox, T. Keith, M. A. Al-Laham, C. Y. Peng, A. Nanayakkara, M. Challacombe, P. M. W. Gill, B. Johnson, W. Chen, M. W. Wong, C. Gonzalez and J. A. Pople, *GAUSSIAN 09 (Revision A.02)*, Gaussian Inc., Wallingford, U.S.A., 2009.

25 M. Jędrzejewski, L. Komorowski and P. Ordon, *J. Mol. Model.*, 2013, **19**, 4203–4207.

26 P. Ordon and A. Tachibana, *J. Chem. Phys.*, 2007, **126**, 234115.

27 P. Ordon and A. Tachibana, *J. Mol. Model.*, 2005, **11**, 312–316.

28 B. Herrera and A. Toro-Labbé, *J. Phys. Chem. A*, 2004, **108**, 1830–1836.

29 S. Gutiérrez-Oliva, B. Herrera, A. Toro-Labbé and H. Chermette, *J. Phys. Chem. A*, 2005, **109**, 1748–1751.